Appl. Phys. B 34, 129–137 (1984)

Applied Physics B Photophysics and Laser Chemistry

Transient Orientational Grating Technique for Investigations of Fast Molecular Relaxation Processes

D. Kühlke*

Department of Physics, Friedrich-Schiller-University, DDR-6900 Jena, German Democratic Republic

Received 28 November 1983/Accepted 30 March 1984

Abstract. A theoretical description of a three-pulse transient grating technique is given where the pump pulses form orientational gratings. Including energy relaxation and angular reorientation the temporal behavior of the diffraction efficiency and energy transmission is discussed with respect to the dependence on the corresponding rate constants and the results are compared with experimental data for Rh6G and RhB. The polarization plane of the pulse diffracted by the grating is found to be rotated in dependence on its initial polarization.

PACS: 33.50, 42.10, 42.60

Laser-induced transient gratings have been observed in a wide variety of materials such as plasmas, dye solutions and semiconductors [1]. Since the grating lifetime is dependent upon the material properties laser-induced gratings can be used to determine important material characteristics. Indeed, three-pulse transient grating techniques have been used to measure properties of a number of systems, as e.g. relaxation constants in dye solutions [2, 3], surface recombination velocities and diffusion constants in semiconductors [4, 5] and energy transport rates in molecular solids [6]. All these grating phenomena are based on a spatial modulation of the ground-state or excited-state population resulting in a modulation of the optical properties of the material (concentration gratings). Because of radiationless transitions the modulation of the absorption is often connected with a modulation of the temperature, and both an absorption grating and a thermal phase grating appear simultaneously. If the inducing light field consists of short laser pulses sound waves can be excited in the sample in addition [1]. In many cases it is difficult to separate the influence of the various gratings. In particular, when using a continuous train of short pulses the contribution of several pulses to the thermal grating may sum up. The occurance of the long living temperature modulation and the gratings resulting from it becomes disadvantageous in investigations of fast relaxation processes by means of transient grating spectroscopy. Thermal gratings can be avoided if orientational gratings produced by two orthogonally polarized pulses are used for such investigations. Recent experimental results of Wu et al. [7] who used the three-pulse transient grating technique with different polarization configurations to study the temporal decay of gratings in liquids illustrate this very impressively. In the case of orthogonally polarized pump pulses the time dependence of the diffracted energy of a delayed probe pulse is mainly determined by the molecular reorientation. In the case of pump pulses with parallel polarization this time dependence is overlayed by an oscillating behavior which has been interpreted to arise from standing sound waves induced by the temperature modulation or by electrostriction.

Orientational gratings are produced by the interference of two orthogonally polarized light fields.

* Present address: University of Essen, D-4300 Essen, Fed. Rep. Germany

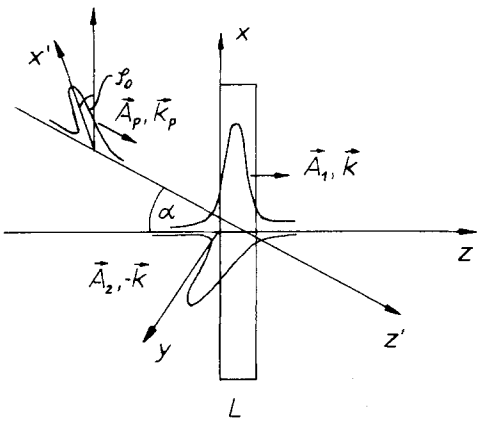

Fig. 1. Scheme of a three-pulse transient grating experiment considered in the text

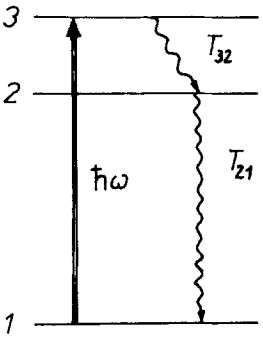

Fig. 2. Energy levels of the absorber

Provided the strength of the resonant excitation depends on the polarization of the field, the ground-state or excited-state population has a preferred orientation that is periodically modulated throughout the material. This occurs even though the total concentration (summed over all orientations) remains spatially uniform, (A.17). Such orientational gratings are produced in molecular systems by selective saturation of molecules with dipole moments aligned with the field. A comperative description of orientational and concentration gratings in degenerate four-wave mixing were given by Wherret et al. [8]. Measurements of the lifetimes of both the gratings in semiconductors were presented by the same authors [9, 10].

In this paper we consider the effect of the orientational gratings formed by two orthogonally polarized strong pump pulses in a molecular liquid on a weak probe pulse. Restricting ourselves to delay times between the pump and probe pulse that are greater than the pulse duration, i.e. neglecting the coherent interaction between the pump and probe pulses, we are able to give an analysis of both the probe pulse direction and background-free direction for arbitrary values of the pump energy and of the small signal absorption (Sect. 1). The results enable us 1) to discuss the dependence of the energy transmission and diffraction efficiency on the pump energy and the small signal absorption, 2) to describe the change in the polarization of the diffracted part of the probe pulse that is caused by the anisotropic preparation of the medium and 3) to work out the dependence of the decay of the energy transmission and of the diffraction efficiency on both the energy relaxation and the orientational relaxation (taken into account by an isotropic rotational diffusion model [11]). The resulting formulae are compared with experimental data obtained by Wu et al. [7]. This item gives the foundation for the determination of relaxation constants from measurements by means of transient absorption and laser-induced orientational grating experiments (Sect. 2). In this sense this method is a valuable complement to picosecond techniques that use the time dependent fluorescence and probe-beam spectra for the investigations of fast molecular relaxation processes [12].

1. Basic Equations

We consider an arrangement, as depicted in Fig. 1. At the time $t=0$ two counter-running, orthogonally polarized pump pulses overlap within the sample of the length L and form an orientational grating in the saturable absorber. After a delay time assumed to be longer than the pulse duration a linearly polarized probe pulse of arbitrary orientation of the polarization plane enters the sample. We look for the characteristics of the transmitted as well as of the diffracted part (background-free direction) of the probe pulse in dependence on the delay time τ and the properties of the absorbing medium. The absorber consists of three-level systems (Fig. 2) with quick vibrational relaxation in the upper electronic level. (For dyes the vibrational relaxation time is in the order of 10^{-12} to 10^{-13} s [17].) Thus the population in the excited vibrational level is neglected. The electromagnetic field interacts with level 3. In particular, the non-resonant interaction with level 2 is neglected. This is justified for a frequency difference between both the levels that is greater than τ_{31}^{-1} and τ_{21}^{-1}. The phase relaxation times τ_{31} and τ_{21} are in the order of 10^{-13} to 10^{-14} s for typical dyes and are assumed to be short in comparison with the pulse duration. With these approximations and the assumption of equal rotational diffusion constants of the ground and the excited state, $D^{(1)}=D^{(2)}=D$, thus $\varrho_{11}(\vartheta,\varphi,\mathbf{r},t)+\varrho_{22}(\vartheta,\varphi,\mathbf{r},t)=1/4\pi$ is valid, the equation of motion of the density matrix including isotropic rotational diffusion provides following

relations

$$\frac{\partial}{\partial t}\varrho_{11}(\vartheta,\varphi,\mathbf{r},t)=DV^2_{\vartheta,\varphi}\varrho_{11}(\vartheta,\varphi,\mathbf{r},t)+\frac{1}{T_{21}}\left[\frac{1}{4\pi}-\varrho_{11}(\vartheta,\varphi,\mathbf{r},t)\right]-\frac{i}{\hbar}\mathbf{d}_{31}\mathbf{E}(\mathbf{r},t)\,\varrho_{13}(\vartheta,\varphi,\mathbf{r},t)+\text{c.c.}, \quad (1)$$

$$\varrho_{31}(\vartheta,\varphi,\mathbf{r},t)=\frac{i\tau_{31}\mathscr{L}}{\hbar}\varrho_{11}(\vartheta,\varphi,\mathbf{r},t)\;\mathbf{d}_{31}\mathbf{E}(\mathbf{r},t); \quad (2)$$

$\mathbf{d}_{31}=d_{31}\mathbf{e}$, with d_{31} being the matrix element of the transition and $\mathbf{e}$ the unit vector of the dipole direction, $\mathscr{L}=[1+i\tau_{31}(\omega-\omega_{31})]^{-1}$ describes the line profile of the transition with the transition frequency ω_{31}, T_{21} and $T_R=1/6D$ are the energy and rotational relaxation times, $V^2_{\vartheta,\varphi}$ is the Laplace operator in spherical coordinates ϑ, φ, and $\mathbf{E}(\mathbf{r},t)$ the electric field strength describing the pulses.

In what follows we separately consider three time intervals, i.e. the preparation of the medium by the pump pulses, the relaxation of the excited medium after the passage of the pump pulses and the probing of the medium by a weak pulse after a delay time τ.

1.1. Pumping of the Absorber

The medium is pumped by an electric field consisting of two counter-propagating plane waves of orthogonal polarization which is represented as

$$\mathbf{E}(z,t)=\tfrac{1}{2}[e^{-i\omega t}\cdot(A_1(z,t)e^{-ikz}\mathbf{e}_1+A_2(z,t)e^{ikz}\mathbf{e}_2)+\text{c.c.}]. \quad (3)$$

$A_1(z,t)\,(A_2(z,t))$ is the slowly varying complex envelope of the pulse propagating in the positive z-direction (negative z-direction), ω, k, the frequency and the wave number of the carrier wave and $\mathbf{e}_i$ the unit vectors in x- $(i=1)$ and y-direction $(i=2)$. We preliminarily neglect the depletion of the pump pulses in the absorber and assume the pulse duration to be short in comparison with the relaxation times T_{21} and T_R, so that the relaxation terms in (1) may be dropped. The depletion of the pump pulses is approximately taken into account in the following section. Using the representation of the unit vector in the dipole direction in the coordinate system determined by the pump pulses (Fig. 1)

$$\mathbf{e}=\cos\varphi\sin\vartheta\mathbf{e}_1+\sin\varphi\sin\vartheta\mathbf{e}_2+\cos\vartheta\mathbf{e}_3 \quad (4)$$

we obtain from (1–4) with the rotating wave approximation

$$\frac{\partial}{\partial t}\varrho_{11}=-\frac{d^2_{31}\tau_{31}}{2\hbar^2}\mathscr{L}^r[|A_1|^2\cos^2\varphi+|A_2|^2\sin^2\varphi+(A_1A_2^*\exp(-2ikz)+\text{c.c.})\sin\varphi\cos\varphi]\sin^2\vartheta\varrho_{11} \quad (5)$$

with the initial condition $\varrho_{11}(\vartheta,\varphi,z,t=-\infty)=1/4\pi$. For the regime after the passage of the pump pulses, the solution of (5) is given by

$$\varrho_{11}=\frac{1}{4\pi}\exp\{-\mathscr{L}^r\sin^2\vartheta[\varepsilon_1\cos^2\varphi+\varepsilon_2\sin^2\varphi+|\varepsilon_{12}|\cos(2kz+\delta)\sin2\varphi]\}, \quad (6)$$

where $\varepsilon_{12}=|\varepsilon_{12}|e^{-i\delta}=d^2_{31}\tau_{31}\int_{-\infty}^{\infty}dt\,A_1A_2^*/2\hbar^2$, $\varepsilon_1=\varepsilon_{11}$, $\varepsilon_2=\varepsilon_{22}$ are the pulse energies normalized to the saturation energy of the absorbing medium and $\mathscr{L}^r=\text{Re}\{\mathscr{L}\}$.

1.2. Relaxation of the Absorber

After the passage of the pump pulses, i.e. in absence of the electric field, (1) reads

$$\frac{\partial}{\partial t}\varrho_{11}(\vartheta,\varphi,z,t)=DV^2_{\vartheta,\varphi}\varrho_{11}(\vartheta,\varphi,z,t)+\frac{1}{T_{21}}\left[\frac{1}{4\pi}-\varrho_{11}(\vartheta,\varphi,z,t)\right], \quad (7)$$

where the initial condition is given by (6) and $V^2_{\vartheta,\varphi}=\sin^{-1}\vartheta\,\partial/\partial\vartheta(\sin\vartheta\,\partial/\partial\vartheta)+\sin^{-2}\vartheta\,\partial^2/\partial\varphi^2$. In what follows the probability of finding the molecul in the ground state independent of its dipole orientation

$$\int_0^{2\pi}d\varphi\int_0^{\pi}d\vartheta\sin\vartheta\varrho_{11}(\vartheta,\varphi,z,t)=\varrho_{11}(z,t) \quad (8)$$

and the weighted averages of the density matrix

$$\int_0^{2\pi}d\varphi\int_0^{\pi}d\vartheta\sin^3\vartheta\varrho_{11}(\vartheta,\varphi,z,t)=\bar{\varrho}_{11}(z,t) \quad (9)$$

$$\int_0^{2\pi}d\varphi\int_0^{\pi}d\vartheta\sin^3\vartheta\begin{pmatrix}\sin2\varphi\\ \cos2\varphi\end{pmatrix}\varrho_{11}(\vartheta,\varphi,z,t)=\begin{pmatrix}\bar{\varrho}'_{11}(z,t)\\ \bar{\varrho}''_{11}(z,t)\end{pmatrix} \quad (10)$$

are required. Using these quantities (7) can be reformulated:

$$\frac{\partial}{\partial t}\varrho_{11}(z,t)=\frac{1}{T_{21}}[1-\varrho_{11}(z,t)], \quad (11)$$

$$\frac{\partial}{\partial t}\bar{\varrho}_{11}(z,t)=\frac{2}{3}\left[\frac{1}{T_R}\varrho_{11}(z,t)+\frac{1}{T_{21}}\right]-\bar{\varrho}_{11}(z,t)\Gamma, \quad (12)$$

$$\frac{\partial}{\partial t}\begin{pmatrix}\bar{\varrho}'_{11}(z,t)\\ \bar{\varrho}''_{11}(z,t)\end{pmatrix}=-\Gamma\begin{pmatrix}\bar{\varrho}'_{11}(z,t)\\ \bar{\varrho}''_{11}(z,t)\end{pmatrix}, \quad (13)$$

with $\Gamma = 1/T_{21} + 1/T_R$. The solution of (11–13) is given by

$$\varrho_{11}(z,t) = 1 + e^{-t/T_{21}}[\varrho_{11}(z,0) - 1], \tag{14}$$

$$\bar{\varrho}_{11}(z,t) = \bar{\varrho}_{11}(z,0)e^{-\Gamma t} + \tfrac{2}{3}[1 - e^{-\Gamma t} + [\varrho_{11}(z,0) - 1](e^{-t/T_{21}} - e^{-\Gamma t})], \tag{15}$$

$$\begin{pmatrix} \bar{\varrho}'_{11}(z,t) \\ \bar{\varrho}''_{11}(z,t) \end{pmatrix} = \begin{pmatrix} \bar{\varrho}'_{11}(z,0) \\ \bar{\varrho}''_{11}(z,0) \end{pmatrix} e^{-\Gamma t}. \tag{16}$$

$\varrho_{11}(z,0)$, $\bar{\varrho}_{11}(z,0)$, $\bar{\varrho}'_{11}(z,0)$, $\bar{\varrho}''_{11}(z,0)$ are the weighted averages, according to (8–10), taken from the initial value (6).

1.3. Behavior of the Probe Pulse

The electric field $\mathscr{E}(\mathbf{r}, t)$ of the probe pulse described by the wave equation

$$V^2\mathscr{E} - \frac{1}{v^2}\frac{\partial^2 \mathscr{E}}{\partial t^2} = \mu_0 \frac{\partial^2 \mathbf{P}}{\partial t^2} \tag{17}$$

consists of a part travelling in the probe pulse direction (denoted by the index p) and a part caused by diffraction from the orientational grating (index d)

$$\mathscr{E}(r,t) = \tfrac{1}{2}e^{-i\omega_p t}[\mathbf{A}_p(\mathbf{r},t)e^{i\mathbf{k}_p\mathbf{r}} + \mathbf{A}_d(\mathbf{r},t)e^{i\mathbf{k}_d\mathbf{r}}] + \text{c.c.} \tag{18}$$

with ω_p, $\mathbf{k}_{p,d}$, and v being the frequency, the wave vectors and the velocity of light, respectively. The polarization $\mathbf{P}(\mathbf{r}, t)$ of the medium is determined by the sum of the contribution of all molecular dipoles

$$P_i(r,t) = \varepsilon_0 \sum_{j=1}^{3} \chi_{ij}\mathscr{E}_j(\mathbf{r},t) = n\int d\Omega\, d_{31i}(\Omega)\,\varrho_{31}(\Omega,\mathbf{r},t,\tau), \tag{19}$$

with n being the particle number density. Ω stands for the spherical coordinates. If the probe pulse is weak enough to neglect population changes the elements of the susceptibility tensor χ_{ij} can be immediately deduced by inserting (2) with (18) into (19):

$$\chi_{ij}(r,\tau) = \frac{in\tau_{31}d_{31}^2}{\varepsilon_0\hbar}\mathscr{L}(\omega_p - \omega_{31}) \cdot \int d\Omega \varrho_{11}(\Omega,\mathbf{r},\tau)\, e_i(\Omega)\, e_j(\Omega), \tag{20}$$

where $e_i(\Omega)$ is the i-th component of the unit vector in the dipole direction. Substituting (18, 19) into the wave equation (17), neglecting second derivatives of the slowly varying quantities $\mathbf{A}_{p,d}$ and using $\partial^2\mathbf{P}/\partial t^2 \simeq -\omega_p{}^2\mathbf{P}$ we find the coupled set of the equations of motion for the components of the complex field envelopes

$$\frac{1}{v_g}\frac{\partial A_{pi}}{\partial t} + \sum_{j=1}^{3}\frac{k_{pj}}{k_p}\frac{\partial A_{pi}}{\partial x_j} = -\sum_{j=1}^{3}(r_{ij}^{(-)}A_{dj} + t_{ij}A_{pj}), \tag{21}$$

$$\frac{1}{v_g}\frac{\partial A_{di}}{\partial t} + \sum_{j=1}^{3}\frac{k_{dj}}{k_p}\frac{\partial A_{di}}{\partial x_j} = -\sum_{j=1}^{3}(t_{ij}A_{dj} - r_{ij}^{(+)}A_{pj}), \tag{22}$$

where

$$r_{ij}^{(\pm)}(\tau) = -\frac{i\omega_p}{2v_g}\langle\chi_{ij}(\tau)\exp(\pm 2ik_{p3}z)\rangle, \tag{23}$$

$$t_{ij}(\tau) = -\frac{i\omega_p}{2v_g}\langle\chi_{ij}(\tau)\rangle. \tag{24}$$

$\langle\ \rangle$ denotes the spatial average over some wavelengths, $k_p = |\mathbf{k}_p|$ and v_g is the group velocity. A known probe pulse enters the medium at $z = 0$, i.e.

$$A_p(0,t) = A_0(t), \tag{25}$$

where $A_0(t)$ is a prescribed function. The diffracted wave is generated in the medium, not introduced from the right, thus at $z = L/\cos\alpha$ (α being the angle between the pump and probe pulse direction), i.e.,

$$A_d(z = L/\cos\alpha) = 0. \tag{26}$$

Equations (21, 22) and the boundary conditions (25, 26) completely describe the response of the absorber prepared by the pump pulses on a probe pulse after a delay τ. In deriving (21, 22) we have used that χ_{ij} has only a periodic z-dependence and that $k_{d1,2} = k_{p1,2}$ and $k_{d3} = -k_{p3}$. The fundamental period of χ_{ij} is π/k, compare (6 and 20), and therefore the spatial average in (23) provides only an essential contribution if

$$k_{p3} = k_p\cos\alpha = \pm k. \tag{27}$$

This is the well-known Bragg-condition. In what follows we assume this condition to be satisfied. The integration over the spherical coordinates in (19) has to be carried out in a coordinate system x', y', z', determined by the geometry of the probe pulse. For the sake of clarity, we consider only small angles between the pump and probe pulse direction ($\cos\alpha \approx 1$). Then the z- and z'-axis nearly coincide and the x'-axis is determined by the orientation of the polarization of the probe pulse. In this coordinate system the unit vector of the dipole direction has the form

$$\mathbf{e}(\vartheta,\varphi) = \cos(\varphi+\varphi_0)\sin\vartheta\mathbf{e}'_1 + \sin(\varphi+\varphi_0)\sin\vartheta\mathbf{e}'_2 + \cos\vartheta\mathbf{e}'_3 \tag{28}$$

with φ_0 being the angle between the x- and x'-axis (Fig. 1). On inserting (28) into (20) we are led to the weighted averages of ϱ_{11}, Eqs. (8–10). Substituting the expressions for these quantities (14–16) into (23 and 24) we can calculate the matrix elements r_{ij}, t_{ij} (Appendix). With the simplifications $\varepsilon_1 = \varepsilon_2$ (equal energy of the

counterpropagating pulses) and $\delta=0$ we find

$$r_{ij}^{(\pm)}=r_{ij}=\tfrac{1}{2}rn\sigma(\omega_p-\omega_{31})\,\mathrm{e}^{-\Gamma\tau}\begin{pmatrix}\sin 2\varphi_0 & -\cos 2\varphi_0 & 0\\ -\cos 2\varphi_0 & -\sin 2\varphi_0 & 0\\ 0 & 0 & 0\end{pmatrix}, \tag{29}$$

$$t_{ij}=\tfrac{1}{2}n\sigma(\omega_p-\omega_{31})\,\mathrm{e}^{-\Gamma\tau}F(\tau)\begin{pmatrix}1 & 0 & 0\\ 0 & 1 & 0\\ 0 & 0 & \dfrac{\langle\varrho_{11}\rangle-2\langle\bar{\varrho}_{11}\rangle+F(\tau)}{F(\tau)}\end{pmatrix}, \tag{30}$$

where $\sigma(\omega_p-\omega_{31})=\sigma_0\mathscr{L}(\omega_p-\omega_{31})$, $\sigma_0=(d_{31}^2\tau_{31}\omega)/\varepsilon_0 v_g\hbar$ is the absorption cross section in the centre of the absorption line and

$$F(\tau)=\tfrac{1}{2}\{\langle\bar{\varrho}_{11}\rangle+\tfrac{2}{3}[\mathrm{e}^{\Gamma\tau}-\mathrm{e}^{\tau/T_R}-\langle\varrho_{11}\rangle(1-\mathrm{e}^{\tau/T_R})]\}. \tag{31}$$

The quantities $\langle\varrho_{11}\rangle$, $\langle\bar{\varrho}_{11}\rangle$, and r are given in the Appendix [(A.5, 6) and for small pump energies, $\varepsilon\ll 1$, (A.8–10)].[1]

Equations (21, 22) with (27, 29, and 30) reduce to a set of four coupled differential equations. Introducing the new variables $\eta=t-z/v_g$, $\zeta=z$ in (21) and $\eta=t-(L-z)/v_g$, $\zeta=z$ in (22) and assuming, in addition, the sample depth to be small compared with the pulse length (i.e., time-of-flight effects are excluded) we obtain

$$\frac{\partial}{\partial\zeta}A_{pi}(\eta,\zeta)=-\sum_{j=1,2}[t_{ij}A_{pj}(\eta,\zeta)+r_{ij}A_{dj}(\eta,\zeta)], \tag{32}$$

$$\frac{\partial}{\partial\zeta}A_{di}(\eta,\zeta)=\sum_{j=1,2}[r_{ij}A_{pj}(\eta,\zeta)+t_{ij}A_{dj}(\eta,\zeta)],\quad i=1,2 \tag{33}$$

with the boundary condition

$$A_{p1}(\eta,0)=A_0(\eta),\ A_{p2}(\eta,0)=A_{p3}(\eta,0)=A_{di}(\eta,L)=0. \tag{34}$$

In (32 and 33) the coefficients r_{ij} and t_{ij} generally are dependent on ζ due to the depletion of the pump pulses in the absorber. We neglect this spatial dependence by replacing $\varepsilon_1(\zeta)$, $\varepsilon_2(\zeta)$, and $|\varepsilon_{12}(\zeta)|$ in (6) by its mean values (Sect. 2.1). With this approximation and the assumption of equal energies of the incident pulses, i.e. $\varepsilon_1=\varepsilon_2$, the solution of (32–34) is found to be

$$A_{p1}(\eta,L)=A_0(\eta)\,[F(\tau)^2-r^2]^{1/2}\cdot\{(F(\tau)^2-r^2)^{1/2}\cosh[\kappa G(\tau)]+F(\tau)\sinh[\kappa G(\tau)]\}^{-1} \tag{35}$$

$$\begin{pmatrix}A_{d1}(\eta,0)\\ A_{d2}(\eta,0)\\ A_{d3}(\eta,0)\end{pmatrix}=\begin{pmatrix}\sin 2\varphi_0\\ -\cos 2\varphi_0\\ 0\end{pmatrix}A_0(\eta)r\sinh[\kappa G(\tau)]\cdot\{[F(\tau)^2-r^2]^{1/2}\cosh[\kappa G(\tau)]+F(\tau)\sinh[\kappa G(\tau)]\}^{-1}, \tag{36}$$

where $G(\tau)=\mathrm{e}^{-\Gamma\tau}(F(\tau)^2-r^2)^{1/2}$ and $\kappa=\kappa^r+\mathrm{i}\kappa^i=n\sigma(\omega_p-\omega_{31})L/2$ the complex absorption coefficient. With the definition of the energy transmission

$$T=\int_{-\infty}^{\infty}d\eta|A_p(\eta,L)|^2\Big/\int_{-\infty}^{\infty}d\eta|A_0(\eta)|^2 \tag{37}$$

and of the diffraction efficiency

$$R=\int_{-\infty}^{\infty}d\eta|A_d(\eta,0)|^2\Big/\int_{-\infty}^{\infty}d\eta|A_0(\eta)|^2 \tag{38}$$

we have

$$R=r^2\{\cosh[2\kappa^rG(\tau)]-\cos[2\kappa^iG(\tau)]\}\cdot\{[2F(\tau)^2-r^2]\cosh[2\kappa^rG(\tau)]+2F(\tau)\,[F(\tau)^2-r^2]^{1/2}\sinh[2\kappa^rG(\tau)]-r^2\cos[2\kappa^iG(\tau)]\}^{-1}, \tag{39}$$

$$T=2[F(\tau)^2-r^2]\,\{[2F(\tau)^2-r^2]\cosh[2\kappa^rG(\tau)]+2F(\tau)\,[F(\tau)^2-r^2]^{1/2}\sinh[2\kappa^rG(\tau)]-r^2\cos[2\kappa^iG(\tau)]\}^{-1}. \tag{40}$$

Equations (35, 36, 39, and 40) are the starting point for the following discussions. It should be noted that the case of purely dispersive media can be formally found by setting $\kappa^r=0$ in (39, 40). Only in this case the relation $R+T=1$ is valid.

2. Discussion of the Results

2.1. Dependence of the Diffraction Efficiency and the Energy Transmission on the Pump Energy and Small-Signal Absorption

In deriving (35–40) the depletion of the pump pulses within the absorber has been neglected. This is, of course, only a rough approximation. The depletion of the pump pulses may be taken into account

[1] It should be noted that the results (29–31) agree with those obtained with a simplified model of the rotational relaxation where the diffusion term $D\nabla^2_{\vartheta,\varphi}\varrho_{11}(\vartheta,\varphi,z,t)$ in (7) is replaced by a phenomenological relaxation term $6D(\varrho_{11}(\vartheta,\varphi,z,t)/4\pi-\varrho_{11}(z,t))$. Such a term was used by Penzkofer and Falkenstein [13] for the description of the probe transmission in excitation-probe experiments [14]. In particular, the time dependence of the weighted averages $\bar{\varrho}_{11}(z,t)$, Eq. (15), $\langle\bar{\varrho}'_{11}(z,t)\rangle$ and $\langle\bar{\varrho}''_{11}(z,t)\rangle$ coincide for both the models

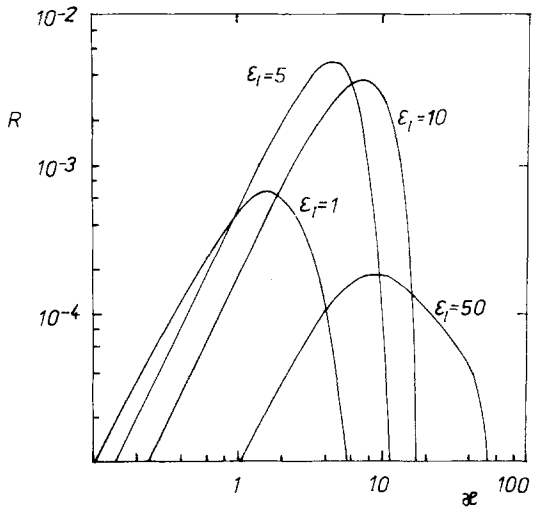

Fig. 3. Diffraction efficiency R versus small-signal absorption κ for different values of the energy of the incident pulses ($\tau=0$, $(\omega_p-\omega_{31})=0$)

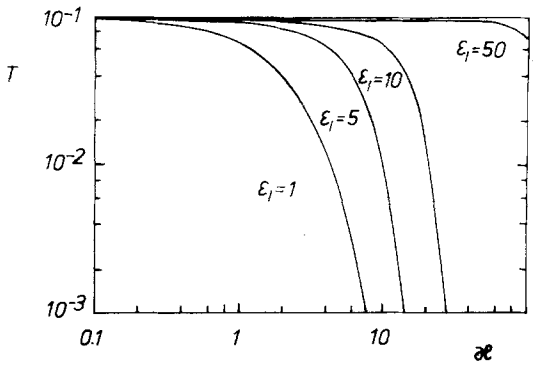

Fig. 4. Energy transmission T versus small-signal absorption κ for different values of the energy of the incident pulses

subsequently in an approximative way if ε and $|\varepsilon_{12}|$ are regarded as mean values obtained by averaging the pulse energy over the sample length. The spatial variation of the pulse energy may be calculated by means of a simple model. For this we assume that the two pump pulses polarized perpendicular to each other interact with two independent reservoirs of absorber molecules. In particular, this includes the neglection of the coherent interaction between the counterrunning pump pulses (self-diffraction) and of the influence of the angular distribution of the molecular dipoles. The rate equations describing this model

$$\frac{\partial N_1}{\partial\zeta}=-\frac{1}{2}\sigma n\varrho_{11}^{(1)}N_1,\quad \frac{\partial N_2}{\partial\zeta}=+\frac{1}{2}\sigma n\varrho_{11}^{(2)}N_2, \tag{41}$$

$$\frac{\partial\varrho_{11}^{(i)}}{\partial\eta}=-N_i\varrho_{11}^{(i)}\quad (i=1,2), \tag{42}$$

where $N_i=d_{31}^2\tau_{31}|A_i|^2/2\hbar^2$ is proportional to the photon flux, have the solution [18]

$$\begin{aligned}&N_1(\zeta,\eta)\\&=N_1(0,\eta)\{1+\exp[-\varepsilon_I(\eta)][\exp(\sigma n\zeta/2)-1]\}^{-1},\\&N_2(\zeta,\eta)=N_1(L-\zeta,\eta),\end{aligned} \tag{43}$$

where $N_1(0,\eta)=N_2(L,\eta)$ and $\varepsilon_I(\eta)=\int_{-\infty}^{\eta}d\eta' N_1(0,\eta')$, i.e. $\varepsilon_I=\varepsilon_I(\eta\to\infty)$ is the normalized energy of the incident pulse. From (43) we may deduce the normalized pulse energies

$$\begin{aligned}\varepsilon_1(\zeta)&=\int_{-\infty}^{\infty}d\eta N_1(\zeta,\eta)\\&=\ln\{1+\exp(-\sigma n\zeta/2)[\exp(\varepsilon_I)-1]\},\\\varepsilon_2(\zeta)&=\varepsilon_1(L-\zeta)\end{aligned} \tag{44}$$

and

$$\begin{aligned}|\varepsilon_{12}(\zeta)|&=\int_{-\infty}^{\infty}d\eta[N_1(\zeta,\eta)N_2(\zeta,\eta)]^{1/2}\\&=\ln\left\{\left(\cosh\left(\frac{\kappa}{2}-x\right)+\exp\left(-\frac{\kappa}{2}\right)[\exp(\varepsilon_I)-1]\right.\right.\\&\quad+\left\{1+2\exp\left(-\frac{\kappa}{2}\right)[\exp(\varepsilon_I)-1]\cosh\left(\frac{\kappa}{2}-x\right)\right.\\&\quad\left.\left.+\left[\exp\left(-\frac{\kappa}{2}\right)\{\exp(\varepsilon_I)-1\}^2\right]^{1/2}\right)\right.\\&\quad\left.\cdot\left[1+\cos\left(\frac{\kappa}{2}-x\right)\right]^{-1}\right\},\end{aligned} \tag{45}$$

where $x=\sigma n\zeta/2$ and $\kappa=nL/2$. The quantities ε and $|\varepsilon_{12}|$ occurring in (6) are obtained by averaging (44 and 45) over the sample length

$$\varepsilon_1=\varepsilon_2=\varepsilon=\int_0^L d\zeta\varepsilon_1(\zeta)/L,\ |\varepsilon_{12}|=\int_0^L d\zeta|\varepsilon_{12}(\zeta)|/L. \tag{46}$$

In Figs. 3 and 4 the dependence of the diffraction efficiency and of the energy transmission on the small-signal absorption are depicted. The curves numerically calculated from (39 and 40) with (A.5, 6), and (46) allow to deduce some interesting aspects. In the range of κ where the diffraction efficiency nearly exponentially grows with increasing small-signal absorption, for $\varepsilon_I>1$, R decreases with increasing energy of the pump pulses at values of κ kept fixed. This becomes more distinct with increasing ε_I. In this range the mean pulse energy in the absorber exceeds the saturation energy and the spatial population modulation deviates from a sinusoidal shape. This deviation which becomes stronger with increasing energy reduces the diffraction efficiency [18]. In the range of κ where the penetration depth of the pump pulses becomes smaller than the absorber length the counter-running pulses only incompletely overlap and with increasing κ $|\varepsilon_{12}|$ decreases very rapidly in comparison with ε. This is the

reason for the rapid decrease of the diffraction efficiency beyond its maximum in the range of $\varepsilon_I < 10$. In the range of κ where R goes beyond its maximum the energy transmission begins to fast decrease with growing small-signal absorption (Fig. 4). In contrast to this the curves for $\varepsilon = 50$ show that the diffraction efficiency already decreases for values of κ where $T \simeq 1$. In this region of strong saturation the direct part of the interfering field of the pump pulses can cause an almost complete bleaching of the absorber in the range where ε begins to differ noticeably from $|\varepsilon_{12}|$ ($\varepsilon > |\varepsilon_{12}|$). This leads to a vanishing modulation of the absorber population. For this reason the maxima of the diffraction efficiency decrease with increasing κ in the range of $\varepsilon_I \gtrsim 10$.

2.2. *Dependence on the Relaxation Rates*

An essential goal of the short-pulse spectroscopy is to determine relaxation rates as, e.g., the energy and the rotational relaxation rates in liquids. Eqs. (39 and 40) show that R and T depend on these rates in a different way. For this reason the simultaneous measurement of the probe and background-free signal should be advantageous for an exact determination of both the relaxation rates. For example, in the low absorption range, $|\kappa| \ll 1$,

$$R \simeq r^2 \exp(-2\Gamma\tau)[(\kappa^r)^2 + (\kappa^i)^2], \tag{47}$$

$$T \simeq 1 - 2F(\tau)\kappa^r \exp(-\Gamma\tau), \tag{48}$$

it is obvious that R decays with a rate $\Gamma = 1/T_{21} + 1/T_R$ which makes impossible a distinction between both the rates without additional assumptions. The decay of T determined by $F(\tau)$, cf. (31), depends in a more complicated manner on the rates Γ, $1/T_{21}$, $1/T_R$.
In the strong absorption range, i.e. $\cosh[2\kappa^r G(\tau)] \simeq \exp[2\kappa^r G(\tau)]/2 \gg 1$, which leads to

$$R \simeq \left(\frac{r}{F(\tau)}\right)^2 \left\{2 + 2\left[1 - \left(\frac{r}{F(\tau)}\right)^2\right]^{1/2} - \left(\frac{r}{F(\tau)}\right)^2\right\}^{-1} \tag{49}$$

$$T \simeq \exp[-2\kappa^r G(\tau)]\left[1 - \left(\frac{r}{F(\tau)}\right)^2\right] \cdot \left\{2 + 2\left[1 - \left(\frac{r}{F(\tau)}\right)^2\right]^{1/2} - \left(\frac{r}{F(\tau)}\right)^2\right\}^{-1}, \tag{50}$$

the τ-dependence of R is mainly determined by $[r/F(\tau)]^2$ and that of T by $\exp[-2\kappa^r G(\tau)]$. In the case of $[r/F(\tau)]^2 \ll 1$ Eq. (49) with (31) gives

$$R = \left(\frac{3}{2} \frac{r \exp(-\Gamma\tau)}{1 - (1 - \langle\varrho_{11}\rangle) e^{-\tau/T_{21}} \left(1 - e^{-\tau/T_R} \frac{3\langle\bar{\varrho}_{11}\rangle/2 - \langle\varrho_{11}\rangle}{1 - \langle\varrho_{11}\rangle}\right)}\right)^2. \tag{51}$$

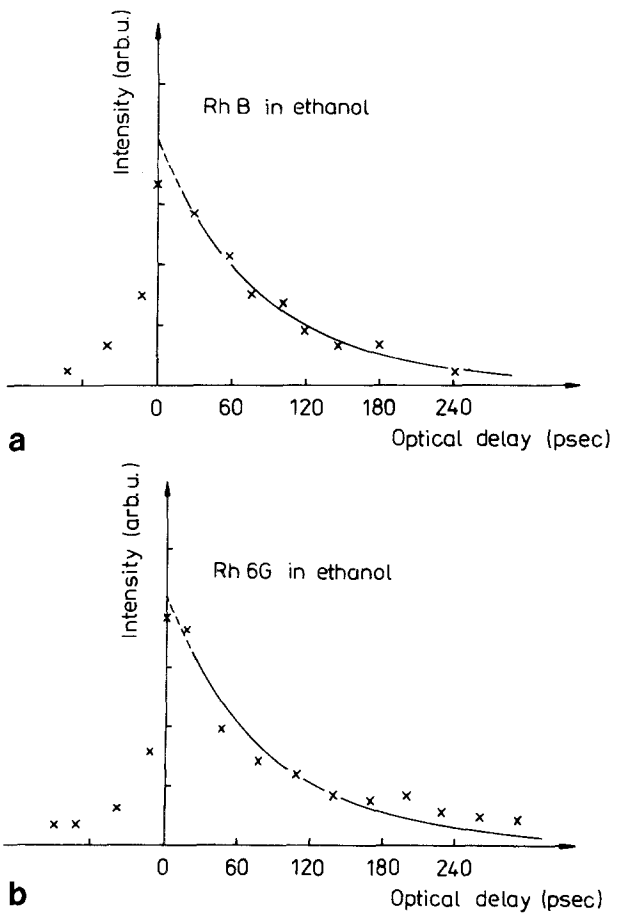

Fig. 5a and b. Dependence of the intensity of the diffracted pulse on the optical delay for solutions of (a) RhB and (b) Rh6G in ethanol (10^{-3} mol/l). x denotes the measured points of Wu et al. [7] for pump pulses with orthogonal polarization. The solid line shows the theoretical dependence obtained by fitting (51) with $1/T_{21} \ll 1/T_R$ to these points [$T_R = 192$ ps, $\langle\bar{\varrho}_{11}\rangle/\langle\varrho_{11}\rangle = 0.56$ (a) and $T_R = 238$ ps, $\langle\bar{\varrho}_{11}\rangle/\langle\varrho_{11}\rangle = 0.43$ (b)]. The dashed part indicates the range where (51) is not valid

The formulae for the temporal behavior of the diffraction efficiency, (39, 47, 49 or 51) may be compared with the experimental results of Wu et al. [7] for the case of orthogonally polarized pump pulses. The experimental conditions of their investigations of the absorbing liquids rhodamine 6G and rhodamine B should meet the range of validity of (51). Figure 5a and b show the results obtained by fitting (51) to the measured time dependence of the diffracted energy of a delayed probe pulse in RhB and Rh6G in ethanol, respectively. From Fig. 5a it is obvious that (51) gives an excellent description of the measured temporal development of the diffraction efficiency in RhB,

whereas the agreement between the theoretical and the experimental dependence in Rh6G is not so good (Fig. 5b). Of course, the experimental conditions of [7] are not fully known to us, but one of the reasons for the lesser agreement could be that the model of an isotropic rotator assumed in deriving (39), (40) is only a rough description of the Rh6G molecul. The resulting constants are $T_R = 192$ ps, $\langle \bar{\varrho}_{11} \rangle / \langle \varrho_{11} \rangle = 0.56$ for RhB and $T_R = 238$ ps, $\langle \bar{\varrho}_{11} \rangle / \langle \varrho_{11} \rangle = 0.43$ for Rh6G. From (A.6) it is deduced that, e.g., $\langle \bar{\varrho}_{11} \rangle / \langle \varrho_{11} \rangle = 0.56$ corresponds to a mean value of the normalized pump energy of $\varepsilon = |\varepsilon_{12}| = 1.3$ in the RhB sample. The value of the orientational relaxation time of Rh6G well agrees with those previously measured ($T_R = 270$ ps [15], $T_R = 250$ ps [16]).

2.3. *Polarization of the Diffracted Pulse*

From (36) it is obvious that the diffracted part of a linearly polarized probe pulse generally suffers a rotation of its polarization plane. The amount of this rotation depends on the orientation of the polarization plane of the incident pulse. For example, if the polarization plane of the probe pulse coincides with that of one of the pump pulses, i.e. $\varphi_0 = 0, \pm\pi/2$, the polarization plane of the diffracted part is rotated by $\pi/2$. If, however, the polarization plane of the probe pulse has the same direction as the orientation of one of the orientational gratings, i.e. $\varphi_0 = \pm\pi/4$, the polarization of the diffracted pulse remains unchanged. That means, for $0 \leqq |\varphi_0| \leqq \pi/4$ every orientation of the polarization plane of the diffracted pulse can be obtained. This behavior is caused by the fact that the pump pulses produce two orientational gratings with a orientation of $\pi/4$ and $-\pi/4$ in the coordinate system determined by the pump pulses (Fig. 1). The maxima of the two gratings are mutually shifted by $\lambda/4$ and, therefore, the components of the probe pulse diffracted by the two gratings suffer a phase difference of $\pi/2$ which leads to the rotation of the polarization plane of the diffracted part. This behavior may be utilized to a further improvement of the signal-to-noise ratio of the background-free signal.

In conclusion we briefly want to discuss the most essential approximations made in this paper. The assumption of a delay time longer than the pulse duration includes the neglection of contributions due to the coherent interaction between the pump and probe pulse (four-wave mixing) and hence enables a solution for arbitrary values of the pump energy and the small-signal absorption. The results are reasonably applicable if the pulse durations are short compared with the relaxation times under investigation.

The model used in (1 and 7) for the description of the rotational diffusion of the molecules contains two essential assumptions. 1) It was assumed that the diffusion constants of the ground and excited state does not differ. Otherwise the relation $\varrho_{11}(\vartheta, \varphi, z, t) + \varrho_{22}(\vartheta, \varphi, z, t) = 1/4\pi$ used for (1) is not valid. This assumption should be justified in the most cases. Recently Reiser and Laubereau [20] have reported measurements of the rotational relaxation rates of the S_0- and S_1-state of phonoxazine dissolved in dioxane and CCl_4, which show a slight difference in the first case (120 and 150 ps) and no difference in the second case. 2) A more restricting assumption is that of an isotropic rotator, i.e. equal axes of the diffusion ellipsoid, $D_x = D_y = D_z = D$. This assumption made for the sake of simplicity is generally not satisfied and must be checked for the actual experimental conditions. (For a detailed discussion of the validity of various models of rotational diffusion compare [12, 14] and references cited there.)

Due to the assumption of a sample depth short compared with the pulse length the equations of motion for the pulse envelope, (21 and 22), have been reduced to stationary ones, (32 and 33). Because of this approximation changes in the shape of the diffracted pulses have been neglected that arise from the influence of time of flight of the probe pulse and from the variation of the grating amplitude in the sample.

The non-resonant interaction of the electromagnetic field of the pulses with level 2 of the three-level system used as model is neglected. This is justified for a frequency difference between both the levels that is greater than the phase relaxation rates of these transitions. Otherwise the influence of the adjacent transition on the dispersion, i.e. on the variation of the refractive index has to be considered. In special wavelength ranges the influence of the resulting phase grating may exceed that of the amplitude grating. Recently Eichler et al. [21] have reported experimental results which show that, e.g., in rhodamine 6G irradiated by pulses of a wavelength of 530 nm the induced phase grating dominates the amplitude grating by an order of magnitude. However, because the relaxation of the corresponding transitions is determined by the same rate constants the time behaviour of the diffraction efficiency is expected to be the same as described above.

Acknowledgement. The author wishes to thank Prof. B. Wilhelmi for valuable discussions.

Appendix

In order to calculate the quantities r_{ij} and t_{ij}, (23 and 24), $\varrho_{11}(\vartheta, \varphi, z)$ given by (6) is expanded into an infinite series

$$\varrho_{11}(\vartheta, \varphi, z) = \frac{A(\vartheta)}{4\pi} \sum_{n=0}^{\infty} \frac{[-B(\vartheta)]^n}{n!} \cos^n(2kz) \sin^n(2\varphi) \tag{A.1}$$

with

$$A(\vartheta) = \exp(-\mathscr{L}^r \varepsilon \sin^2 \vartheta),\ B(\vartheta) = \mathscr{L}^r |\varepsilon_{12}| \sin^2 \vartheta \tag{A.2}$$

and where $\varepsilon_1=\varepsilon_2=\varepsilon$, $\delta=0$ has been assumed. To carry out the integration over φ and z the following relations are used

$$\int_0^{2\pi} d\varphi \sin^m(2\varphi)=\begin{cases}0, & m=2n+1\\ \dfrac{2\pi}{2^{2n}}\binom{2n}{n}, & m=2n\end{cases} \qquad n=1,2,\ldots, \tag{A.3}$$

$$\langle\cos^m(2kz)\rangle=\frac{1}{l}\int_0^l dz\cos^m(2kz)$$

$$=\begin{cases}0, & m=2n+1\\ \dfrac{1}{2^{2n}}\binom{2n}{n}, & m=2n,\end{cases} \tag{A.4}$$

where terms $\sim(nk)^{-1}$ have been neglected. l denotes a length of some periods of k^{-1}. Inserting (A.1) with (A.2) into (23, 24) with (20) and using the relations (A.3 and 4) the results, (29 and 30), are obtained, where

$$r=-\frac{1}{4}\int_0^\pi d\vartheta \sin^3\vartheta A(\vartheta)\sum_{n=1}^{\infty}\frac{B(\vartheta)^{2n-1}}{(2n-1)!}\left[\frac{1}{2^{2n}}\binom{2n}{n}\right]^2, \tag{A.5}$$

$$\begin{pmatrix}\langle\varrho_{11}\rangle\\ \langle\bar{\varrho}_{11}\rangle\end{pmatrix}=\frac{1}{2}\int_0^\pi d\vartheta\begin{pmatrix}\sin\vartheta\\ \sin^3\vartheta\end{pmatrix}A(\vartheta)\sum_{n=0}^{\infty}\frac{B(\vartheta)^{2n}}{(2n)!}\left[\frac{1}{2^{2n}}\binom{2n}{n}\right]^2. \tag{A.6}$$

In particular, one obtains by means of (A.3, 4) the relation

$$\int_0^l dz\cos(2kz)\,\varrho_{11}(z,0)=\int_0^l dz\cos(2kz)\,\bar{\varrho}_{11}(z,0)=0. \tag{A.7}$$

That means, the total ground-state population (summed over all angles) and the weighted ground-state population have no periodic z-dependence, i.e. there is no concentration grating.
In the case of small pump energies, $|\varepsilon_{12}|=\varepsilon\ll 1$, (A.5, 6) can be approximated by

$$r=-\mathscr{L}^r\varepsilon/15, \tag{A.8}$$

$$\langle\varrho_{11}\rangle=1-2\mathscr{L}^r\varepsilon/3, \tag{A.9}$$

$$\langle\bar{\varrho}_{11}\rangle=2(1-4\mathscr{L}^r\varepsilon/5)/3. \tag{A.10}$$

References

1. H.J. Eichler: Opt. Acta **24**, 631 (1977)
2. D.W. Phillon, D.J. Kuizenga, A.E. Siegman: Appl. Phys. Lett. **27**, 85 (1975)
3. A. von Jena: Appl. Phys. B **26**, 1 (1981)
4. K. Jarasiunas, H. Gerritsen: Appl. Phys. Lett. **33**, 190 (1978)
5. C.A. Hoffman, K. Jarasiunas, H. Gerritsen, A. Nurmikko: Appl. Phys. Lett. **33**, 536 (1978)
6. J.R. Salcedo, A.E. Siegman, D.D. Dlott, M.D. Fayer: Phys. Rev. Lett. **41**, 131 (1978)
7. C.K. Wu, P. Agostini, G. Petite, F. Fabre: Opt. Lett. **5**, 67 (1983)
8. B.S. Wherrett, A.L. Smirl, Th. Boggess: IEEE J. QE-**19**, 680 (1983)
9. Th. Boggess, A.L. Smirl, B.S. Wherrett: Opt. Commun. **43**, 128 (1982)
10. A.L. Smirl, Th. Boggess, B.S. Wherrett, G.P. Perryman, A. Miller: IEEE J. QE-**19**, 690 (1983)
11. H.E. Lessing, A. von Jena: In *Laser Handbook*, ed. by M. L. Stitch (North-Holland, Amsterdam 1979) p. 755
12. B. Wilhelmi: Proc. ISLA, Vilnius 1981 (in press)
13. A. Penzkofer, W. Falkenstein: Chem. Phys. Lett. **44**, 547 (1976)
14. H. Wabnitz: Dissertation, Jena (1982)
15. T.J. Chuang, K.B. Eisenthal: Chem. Phys. Lett. **11**, 368 (1971)
16. G.R. Fleming, A.G.W. Knight, J.M. Morris, R.J. Robbins, G.W. Robinson: Chem. Phys. Lett. **51**, 399 (1977)
17. F.P. Schäfer (ed.): *Dye Lasers* (Springer, Berlin, Heidelberg, New York 1977)
18. J. Herrmann, J. Wienecke, B. Wilhelmi: Opt. Quantum Electron. **7**, 331 (1975)
19. D. Kühlke, W. Dietel: Opt. Quantum Electron. **9**, 305 (1977)
20. D. Reiser, A. Laubereau: Chem. Phys. Lett. **92**, 297 (1982)
21. H.J. Eichler, U. Klein, J. Salk, N. Wiese: Verh. DPG (VI) **18**, 465 (1983)